Sustainable Chemical Engineering
http://ojs.wiserpub.com/index.php/SCE/

UNIVERSAL WISER PUBLISHER

Research Article

A Novel Banana Fiber Reinforced Green Composite from Maleated Castor Oil and Linseed Oil

S. H. Kumarage, P. I. Godakumbura*, M. A. B. Prashantha

Department of Chemistry, Faculty of Applied Sciences, University of Sri Jayewardenepura, Gangodawila, Nugegoda, Sri Lanka
E-mail: pahanig@sjp.ac.lk

Received: 4 Septembert 2023; **Revised:** 30 October 2023; **Accepted:** 2 November 2023

Abstract: In recent decades, the consumerist society has recognized the consequences of petrochemicals, hence the interest of scientists has been drawn toward renewable products obtained from biological sources. In this study a novel biocomposite with the use of the least chemicals was fabricated by crosslinking maleated castor oil (MACO) and linseed oil (LO) by free radical polymerization, using benzoyl peroxide (BPO) as the free radical initiator. The significance of this study is that the polymer matrix is derived entirely from vegetable oils with slight modifications. Banana fibers are one of the strongest natural fibers that may be taken from the banana pseudo-stem that is discarded after the fruit is harvested. To convert this post-harvest waste into a value-added product, NaOH-treated banana fibers were used as the reinforcement for the developed composite. The characterization of the fibers and the composites was carried out by performing Fourier-transform infrared spectroscopy (FT-IR), X-Ray diffraction analysis (XRD), Dynamic mechanical analysis, tensile and compressive stress analysis, Scanning electron microscopy (SEM), Thermogravimetric (TG)/ derivative thermogravimetric (DTG) and thermal conductivity analysis. Composites were also analyzed for their water absorptivity and chemical resistivity. The influence of varying banana fiber weights on the composite's mechanical strength was investigated using a dual cantilever flexural test. It revealed that the composite's strength increased with increasing fiber content until 50% (w/w) and then dropped as the fiber content increased further. The maximum tensile strength of the optimum composite was 16.92 ± 4.70 Megapascal (MPa) and the composite was resistant against a compressive force of 4,500 kN without any fractures. The composites' water absorptivity and chemical resistivity tests revealed that increasing the fiber content enhanced the composites' swelling. The composite was acidic and saline water resistant, but not alkaline solution resistant. Additionally, the thermal conductivity measurements of the composite showed that the composite is a thermal insulator. The composite with 50% (w/w) fiber load, 20% (w/w) BPO, 10% (w/w), LO and 20% (w/w) MACO exhibited the best overall performances.

***Keywords*:** green composites, renewable resources, vegetable oils, castor oil, linseed oil, banana fibers, value addition

1. Introduction

Polymer composites have become an essential part of the current materials as they offer a wide range of beneficial properties and are being used in simple domestic equipment to air crafts. To meet human requirements, several synthetic petrochemical-based polymeric products have been developed over time. These man-made polymer materials

DOI: https://doi.org/10.37256/sce.5120243616

using non-renewable raw materials have adversely affected to the natural environment and health. Hence potentially novel approaches that take environmental preservation into account must be created in order to address these severe issues.[1] More research has recently been focused on the development of bio-based materials because of concerns about sustainability, environment, energy, and cost. The use of bio-based polymers reduces the need for synthetic polymers derived from petrochemicals, which is beneficial for the environment across the globe. Biocomposites, where a bio-based polymer matrix is reinforced by natural fibers are known as green composites. Both the matrix and the reinforcement material originate from renewable resources and they can be composted in a nature-friendly manner at the end of life.[2]

Vegetable oils owing to their adaptability, availability, renewability, biodegradability and as a rich source for many different polymers and polymer precursors, have been most widely used as a highly promising alternative to petroleum-based polymers. The chemical and functional properties of the vegetable oil triglycerides can be modified to enhance their properties and usability in varied sectors, such as fuels, lubricants, paints and coating industries, polymer materials, etc.[3-4] Castor oil (CO) is a pale yellow, non-volatile, viscous, non-edible oil with a characteristic odour. The oil is extracted from the seeds of castor plants (*Ricinus communis*) by one or a combination of mechanical and solvent extraction methods. The properties vary with the method of extraction.[5] The chemistry of castor oil is dependent on its high content of ricinoleic acid (90%) with three points of functionalities: the carboxyl group, hydroxyl group and the single unsaturation which can be modified to alter the properties of the oil.[6] Castor oil is extensively used in the polymer industry due to its capability of carrying out versatile chemical modifications.[7] The double bonds of castor oil triglycerides are not reactive enough to take part in free radical polymerization.[8] Hence to provide it with additional reactive double bonds first castor oil was converted to maleated castor oil (MACO) (Figure 1) without any catalysts.[9] Linseed oil (LO), also known as flaxseed oil, is extracted from dried ripened seeds of the flax plant (*Linum usitatissimum*) and the major triglycerides in linseed oil, are linolenic acid (53%), oleic acid (18%), linoleic acid (15%), palmitic acid (6%) and stearic acid (6%).[10] Linseed oil is a drying oil which undergoes polymerization on exposure to air by auto-oxidation and hence is used extensively in paint and coating industries for centuries. Linseed oil is considered one of the triglycerides with the highest average number of double bonds which is beneficial in polymerizing.[11]

Natural fibers are appealing reinforcing materials due to their low cost, nontoxicity, adequate tensile strength, less health risk and potential biodegradability. Due to these properties, natural fibers have been used as an alternative to synthetic fibers as a reinforcing agent.[12] Banana fibers are a readily available natural cellulose fiber source with reasonably excellent mechanical characteristics that have the potential to be employed as a reinforcing component in composites.[13-14] The fibers are extracted from the pseudostem of banana plant which is a residue after harvesting the banana fruit. Hence utilizing this post-harvest waste will ultimately result in transforming large-scale agricultural waste into value-added products.[15-18]

Although there are many vegetable oil-based polymer composites developed, they are majorly based on the epoxidation of vegetable oils which involves several chemicals.[18-19] The aim of this study is to develop a banana fiber-reinforced biocomposite with a matrix derived solely from vegetable oils, employing the least chemicals possible with a simple and convenient methodology. The innovative strategy in this composite manufacturing involves the fabrication of the polymer matrix by only using the least modified vegetable oils without any synthetic polymers. MACO and LO were cross-linked to generate the composite matrix. The only modification for the vegetable oils done was maleating the castor oil simply by heating the oil with maleic anhydride and LO was used as it is. This polymer matrix acts more like an adhesive, adhering the banana fibers together and giving the composite rigidity. Mechanical characteristics, morphological analysis, water absorption, chemical resistance, and thermal properties of the composite were all given special consideration in this work. The green composite developed here showed a promising route to replace petroleum-based composites used in household applications such as panels and thermal insulators. Furthermore, the composite has the potential to be used in impact-bearing applications in the packaging industry.

2. Materials and methodology

2.1 *Materials*

Both industrial grade castor (*Ricinus communis)* oil and linseed (*Linum usitatissimum*) oil obtained from Glorchem

enterprise, Sri Lanka were used as received. Maleic anhydride (Research lab fine chem industries, India, 99%), benzoyl peroxide (BDH Chemical Ltd, England, 25% H_2O stabilized) and sodium hydroxide pellets (Research lab industries, 98%) were used.

2.2 *Fiber extraction, treatment, preparation and characterization*

The banana pseudo stem of *Musa acuminata* (sour banana) was cut and separated into sheaths. The sheaths were then water retted for two weeks and then the pulpy part was scrapped to obtain the fibers. The acquired fibers were then washed and dried well. The fibers were treated with 5% (w/v) NaOH aqueous solution for two hours under ambient conditions (27 °C and atmospheric pressure) and washed well with distilled water until neutral. Then it was well dried in an air oven at 70 °C to remove moisture. The fibers were then cut into small pieces.

ATR-FTIR and X-ray Diffraction (XRD) analysis were carried out for the alkaline-treated fibers and non-treated fibers to confirm the removal of waxy amorphous compounds. The FTIR spectra of all banana fiber samples are recorded on a Thermo Scientific Nicolet S10 FT-IR between 400 cm^{-1} and 4,000 cm^{-1} regions. To ascertain the crystallinity of each fiber specimen and to comprehend the crystallographic nature of the banana fiber samples, XRD is performed. This study was performed on a Rigaku-ultima-iv-X-ray-diffractometer operating at 40 KV and 30 mA with Cu K α (1.141 Å) radiation. Finely cut banana fiber is stored in a sample holder and is continuously scanned at a rate of two degrees per minute within the 5°-70° range. Using the Segal empirical approach, the crystallinity index (X_{cr}) of the fiber was determined with equation 1:

$$X_{cr} = \frac{\left(I_{002} - I_{am}\right)}{I_{002}} \times 100 \quad (1)$$

where I_{002} is the maximum intensity of the peak at 2θ = 22° and I_{am} is the height of the minimum between the 002 and the 101 peaks, which is due to the amorphous region of the sample.

In order to compare the morphological changes of the fiber surfaces, before and after NaOH treatment Scanning Electron Microscopy (SEM) analysis was performed using the Carl ZEISS evo18 model using secondary electron mode at an accelerating voltage of 10 kV.

2.3 *Synthesis of maleated castor oil*

Castor oil and maleic anhydride were reacted in a 1:3 molar ratio at 125 °C with constant mechanical agitation for four hours according to a previously published procedure.[9] The reaction mechanism is shown in Figure 1. The progress of the reaction was monitored by measuring the acid value every hour with increasing viscosity. ATR-FTIR analysis was also carried out at the end of four hours in order to confirm the esterification between the castor oil and maleic anhydride.

2.3.1 *Determination of acid value*

The acid value measures the number of acidic groups in a constituent (such as carboxyl groups) and is represented as the amount of potassium hydroxide (KOH) standard solution needed to neutralize all of the acidic ingredients found in 1 g of oil sample.

Exactly 10.0 g of oil was weighed into a 250 ml conical flask and was mixed with 50 ml of diethyl ether: ethanol (1:1) mixture. It was then titrated with standardized 0.1 M alcoholic KOH using phenolphthalein as an indicator. Titration was triplicated. The acid value was determined using the following equation 2.

$$\text{Acid value} = \frac{56.1 \text{ g mol}^{-1} \times \text{normality of KOH} \times \text{volume of KOH}}{\text{weight of the oil}} \times 100 \quad (2)$$

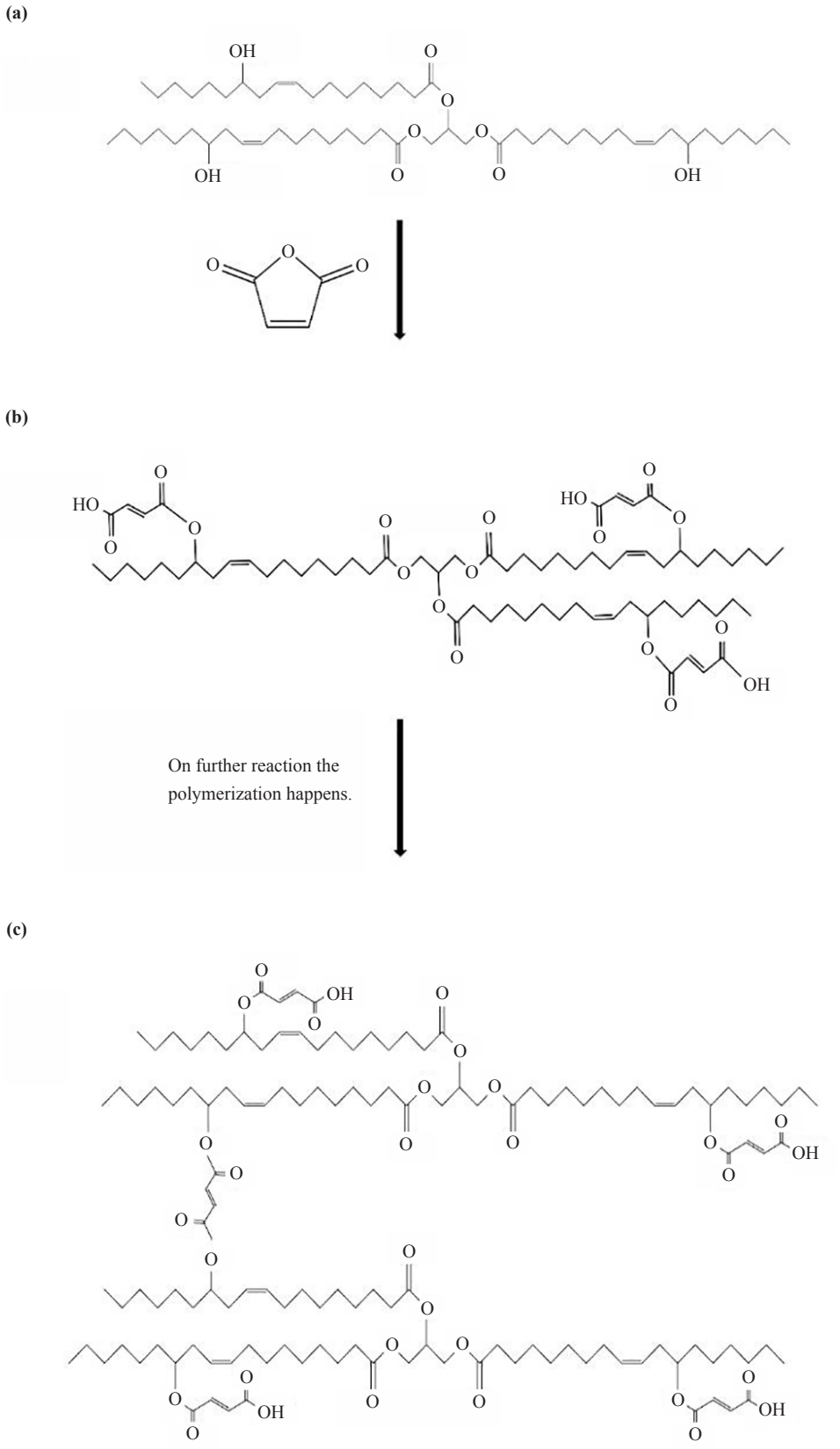

Figure 1. Castor oil triglyceride reacting with maleic anhydride. (a) Castor oil triglyceride. (b) MACO monomer. (c) MACO dimer

2.4 *Synthesis of the composite*

To produce the polymer matrix of the composite LO was mixed with MACO. BPO and fiber was then added to the mixture of MACO and LO. BPO was used as the initiator for the free radical polymerization between LO and MACO.

Initially, the composites were fabricated by changing only the fiber content and MACO as given in Table 1. All four samples were cured in a compression mold at a temperature of 130 °C for 30 minutes at 500 psi.

Table 1. Composition of the samples to evaluate the fiber loading

Sample	Sample composition (w/w) %			
	Fiber content	LO	BPO	MACO[a]
1	30	10	10	50
2	40	10	10	40
3	50	10	10	30
4	60	10	10	20

[a] MACO was added to make the mixture total to 100%

The composite with the optimum fiber loading that provides the best qualities was determined by analyzing the properties of the above four sample composites and was further modified by altering the other content parameters while retaining the fiber content at its optimal level as shown in Table 2 in section 3.3.

2.5 *Characterization of composite*

The-pat-and-weight technique was used to determine the water uptake.[20-21] Each sample was dried in an oven at 50 °C for 24 hours followed by cooling in a desiccator and weighed. The samples were then immersed in 50 mL of distilled water for 24 hours. The weight of the samples was measured in 1-hour time intervals for 5 hours and the last measurement was obtained after 24 hours. The specimens were taken out from the water, quickly wiped with a clean tissue to remove excess water, reweighed and put back in the water. Water absorptivity was determined using the following equation 3.[21] pH of the water samples in which the samples were kept for 24 hours, was measured at the end in to order check if there was any acid or base leaching into the surrounding environment.

$$\text{Water uptake } \% = \frac{W_W - W_{ID}}{W_{ID}} \times 100 \tag{3}$$

where W_W is the wet weight of the sample, W_{ID} is the initial dry weight of the sample.

The samples were dried at the end of 24 hours, and the percentage of water-soluble matter was determined in terms of the weight loss of the samples at the end of 24 hours of immersing the samples in water using the equation 4.[21]

$$\text{Soluble matter } \% = \frac{W_{ID} - W_{FD}}{W_{ID}} \times 100 \tag{4}$$

where W_{FD} is the final dry weight of the sample.

The chemical resistivity of the composites in acidic, alkaline and saline water was determined in terms of the percent chemical swelling. Each sample was well-dried in an oven at 50 °C for 24 hours, cooled in a desiccator and weighed. The samples were then kept in 50 ml of the following solution for 24 hours. [22]

- acidic (2% H_2SO_4) (w/v) solution
- alkaline (2% NaOH) (w/v) solution
- saline (20% NaCl) (w/v) water

The weight of each sample was measured for every hour until 5 hours and the last measurement was obtained after 24 hours. The swelling percentage was determined by the following equation 5.[20]

$$\text{swelling } \% = \frac{W_W - W_{ID}}{W_{ID}} \times 100 \quad (5)$$

The mechanical properties of the composites were analyzed by dynamic mechanical analysis (DMA), and tensile and compressive tests. Dynamic mechanical properties in terms of storage modulus and loss modulus of all the sample composites were determined using the Q800 DMA V21.3 Build 96 instrument in dual cantilever mode. The test was carried out with a frequency of 1 Hz and amplitude of 20 µm over a temperature range of 25 °C to 250 °C. Rectangular specimens of 56 mm × 13 mm × 3 mm were made using a steel mold. Based on the DMA studies the composite with the optimum strength was selected and was tested for its tensile and compression strength using Echo Lab Universal Testing Machine (UTM) model ETM-5 with a load cell of 500 kg operating at a crosshead speed of 0.2 mm/min. For tensile testing, dumbbell-shaped specimens with dimensions of 15 mm × 8 mm × 3 mm were used while for compression testing cylindrical shaped specimens with 30 mm diameter and 10 mm thickness were used. Fractographic analysis of the tensile fractured composite was carried out using SEM images.

The optimum sample was also characterized for its thermal stability by performing thermo gravimetric analysis (TGA) using TA SDT 650. The sample was heated from room temperature to 600 °C at a heating rate of 20 °C/min. Thermal conductivity was also measured using a hot disc thermal constants analyzer (HDT) for the composite with the optimum mechanical and chemical properties.

3. Results and discussion

3.1 *Characterization of banana fibers*

Natural fibers have to be treated in order to enhance the adhesion at the composite interface. The most common way of treating natural fibers is an alkaline treatment using NaOH.[23] This reduces the amorphous and waxy compounds such as lignin, hemicellulose, waxes and oils within the fiber matrix which in return increases the fiber roughness. The increase of fiber roughness increases the fiber-matrix adhesion of the composite.[24] It is reported that the higher the alkaline concentration, the higher the removal of impurities and at very high concentration levels the degradation of the fibers was intense. Also, the alkaline treatment has reduced the water absorption characteristics due to the reduction in hemicellulose.[25] Further it is reported that the composites reinforced with the treated fibers have higher mechanical properties than the composites reinforced with untreated fibers.[26-27]

The ATR-FTIR spectra of treated and untreated fibers were compared in Figure 2. A wide and strong band at 3,339 cm^{-1} was attributed to a vibration extension of the OH groups. The absorption band at 2,921 cm^{-1} was attributed to the extension of the C-H methyl and methylene groups of the fibers.[28] The bands of 1,746 cm^{-1} and 1,631 cm^{-1} can be attributed to the vibration stretching of C = O groups, in particular due to the unconjugated C = O of hemicellulose and conjugated C = O of lignin respectively.[29-30] In addition, peak intensity at 1,247 cm^{-1} attributed to the C-O stretching of acetyl groups in hemicellulose is almost absent in treated fibers.[25] The disappearance of the peak at 1,247 cm^{-1} and the decrease of intensities of the peaks at 1,746 cm^{-1} and 1,631 cm^{-1} in the treated fibers compared to the untreated fibers indicate the impact of the alkaline treatment on the banana fibers in order to lower the lignin and hemicellulose content of the fibers.[25] Moreover the decrease in the intensity of the peak at 1,036 cm^{-1} which is attributed to C-O-C linkage in treated fiber also indicates the removal of adhered lignin/hemicellulose of the banana fibers.[31]

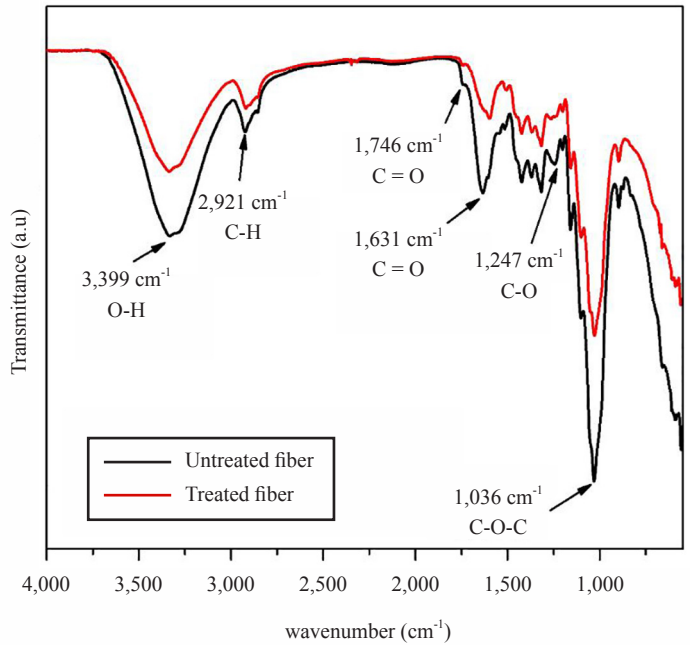

Figure 2. ATR-FTIR spectra of NaOH treated and untreated banana fibers

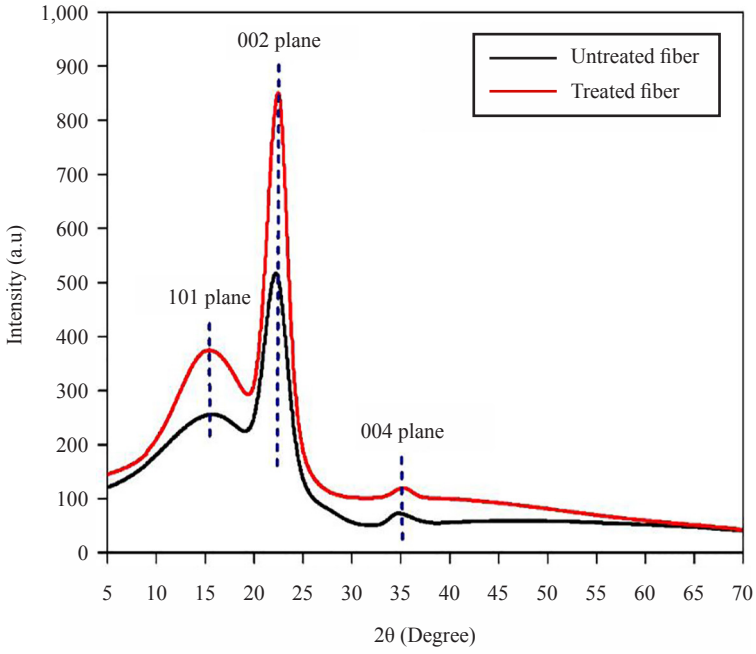

Figure 3. XRD of NaOH treated and untreated banana fibers

A strong peak at 2θ value 15.2° corresponding to the 101 plane, a very intense peak at 2θ value 22.5° corresponding to the 002 plane, and one minor peak at 2θ value 35.2° belonging to the 004 plane characterize the XRD spectra (Figure 3) of the untreated and treated banana fibers. The intensity of these peaks is higher in the treated fibers than in the untreated fibers. The treated and untreated banana fiber specimens have crystallinity indices of 65.5% and 56.4%, respectively which indicate the higher crystallinity of treated fibers. The amorphous materials that have adhered to the fibers have

been eliminated from the fiber surface by the alkali treatment thus increasing the crystallinity index.[31]

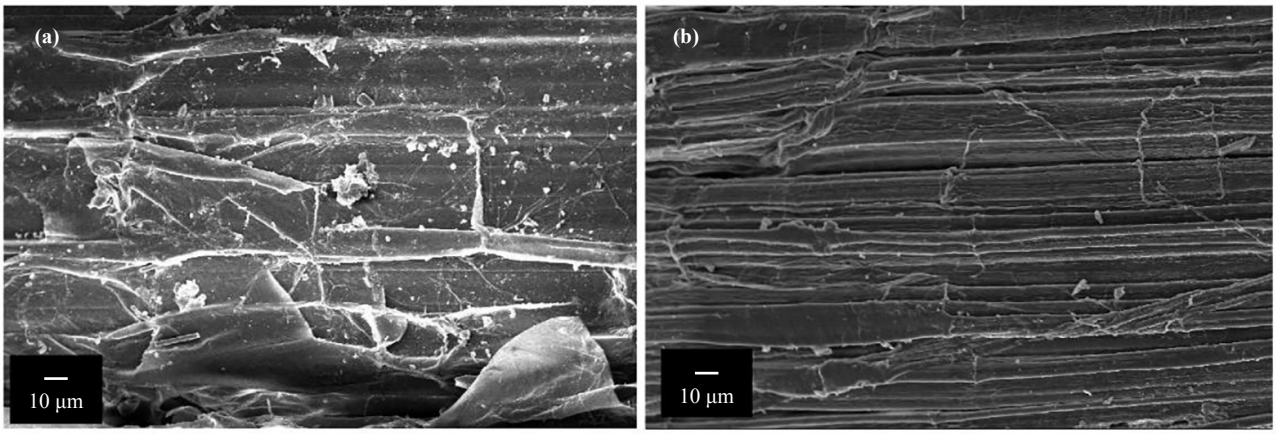

Figure 4. SEM images of (a) untreated banana fibers and (b) NaOH treated banana fibers

Figure 4 displays the SEM pictures of the untreated banana fibers and banana fibers treated with NaOH which further confirmed the removal of non-cellulosic materials from the fibers. They demonstrate that a layer of materials, possibly consisting of lignin, hemicellulose, and other non-cellulosic materials, covers the surfaces of the untreated fibers. NaOH-treated fibers exhibit surface roughness and ridges on the surface of fibers, indicating the removal of non-cellulosic material. Furthermore, it is evident that the tiny, particular contaminants on the fiber's surface have also been stripped from the treated fibers. A better interaction with the matrix will be made possible by the reduction of non-cellulosic material and an increase in the roughness and surface area of the fibers' surface.[32] The length of the cut banana fibers was also determined to be 14.17 ± 4.59 mm using SEM.

3.2 *Characterization of MACO*

3.2.1 *Acid value analysis during the synthesis of MACO*

Figure 5 shows the change in acid value in 1-hour time intervals during the reaction between castor oil and maleic anhydride. The initial higher acid value was due to the presence of free carboxyl groups, mainly from maleic anhydride ring openings. With the progress of the reaction when the polymerization occurs, the number of free carboxylic acid groups decreases as in the reaction scheme shown in Figure 3. Hence the decrease of acid value indicates the decrease of carboxylic acid groups, with the formation of the ester bond between the hydroxyl group of the castor oil and the carboxylic groups of maleic acid.

3.2.2 *The FT-IR analysis of CO and MACO*

The analysis of FTIR peaks confirmed the formation of the ester bond between the hydroxyl groups of castor oil and the carboxyl group of the maleic anhydride. The major changes in the peaks of the spectrum are assigned in the IR spectra shown in Figure 6.

The peak at 1,742 cm^{-1} can be attributed to C = O carbonyl groups. The prominence of the peak at 1,653 cm^{-1} which is assigned to the C = C double bond stretching frequency in MACO depicts the addition of more double bonds to the castor oil. This in turn confirmed the addition of maleic anhydride to the castor oil to produce MACO. The significant increase in the two peaks at 1,241 cm^{-1} and 1,164 cm^{-1} which are attributed to the stretching of the two C-O bonds in the ester bond and the decrease of OH peak at 3,409 cm^{-1} confirmed the formation of the ester bond between the hydroxyl of the castor oil triglyceride and the carboxyl group of maleic acid.[33]

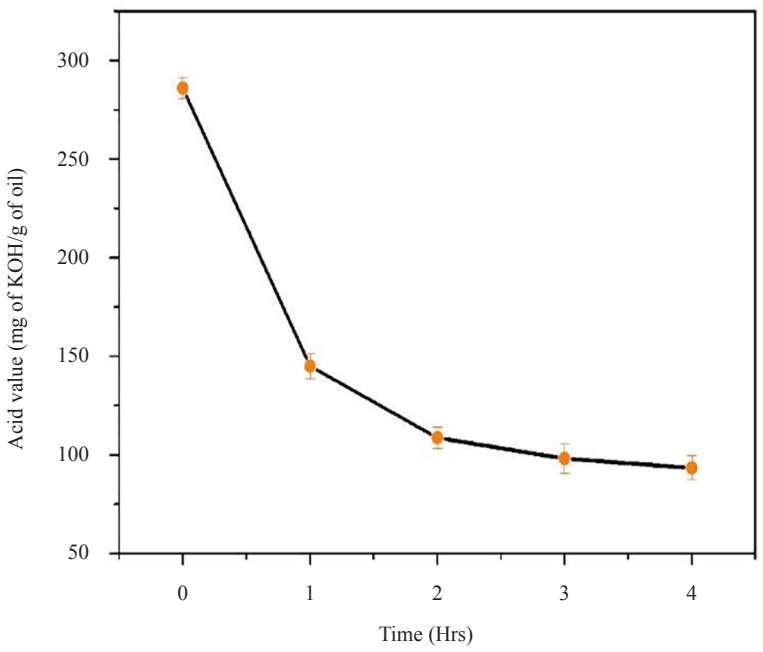

Figure 5. Reduction of acid value with time during the reaction of Castor oil and MA

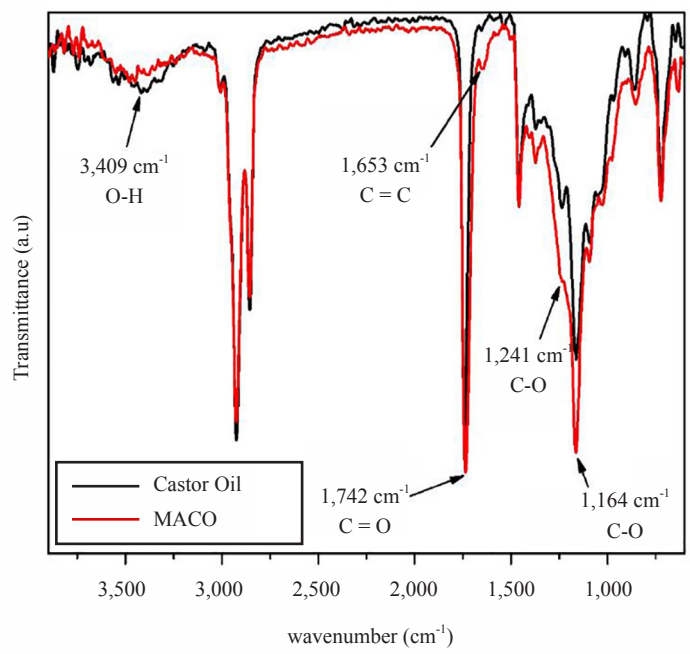

Figure 6. ATR-FTIR spectra of CO and MACO

3.3 *Comparison of mechanical properties*

Initially, the dynamic mechanical properties in terms of storage and loss modulus of the samples with varying fiber content were determined in order to select the optimum fiber content that showed the highest strength. The storage modulus and loss modulus of samples 1 to 4 are shown in Figure 7 (a) and (b) respectively.

The storage modulus interprets elastic nature, which is the ability of a sample to absorb and transfer the stress throughout the matrix without any breakages at a given temperature.[34] With the increase of fiber content of the composite up to 50 w/w in the polymer matrix, the stress transfer ability of the composite upsurges, thus increasing the storage modulus as perceived in Figure 7(a). When the fiber content increased up to 60 w/w the storage modulus showed a drastic decrease, owing to the failure of the effective stress transfer due to incomplete wetting of the fiber by the polymer matrix.[21] As the temperature increases the molecular motions increase with the deterioration of the polymer-filler interaction, moving the molecules away from each other, thus decreasing the stress transfer ability.[35] The hydrogen bonding interactions between polymer and cellulose banana fibers are disrupted at higher temperatures. A number of natural fiber-reinforced composites exhibit a similar pattern in their storage modulus.[36] However with the continuous increase of temperature closer to 130 °C-140 °C , further crosslinking of the polymer matrix starts to occur resulting in strong packing and restricting the movements of the polymer chain molecules in the composite matrix thus increasing the storage modulus.

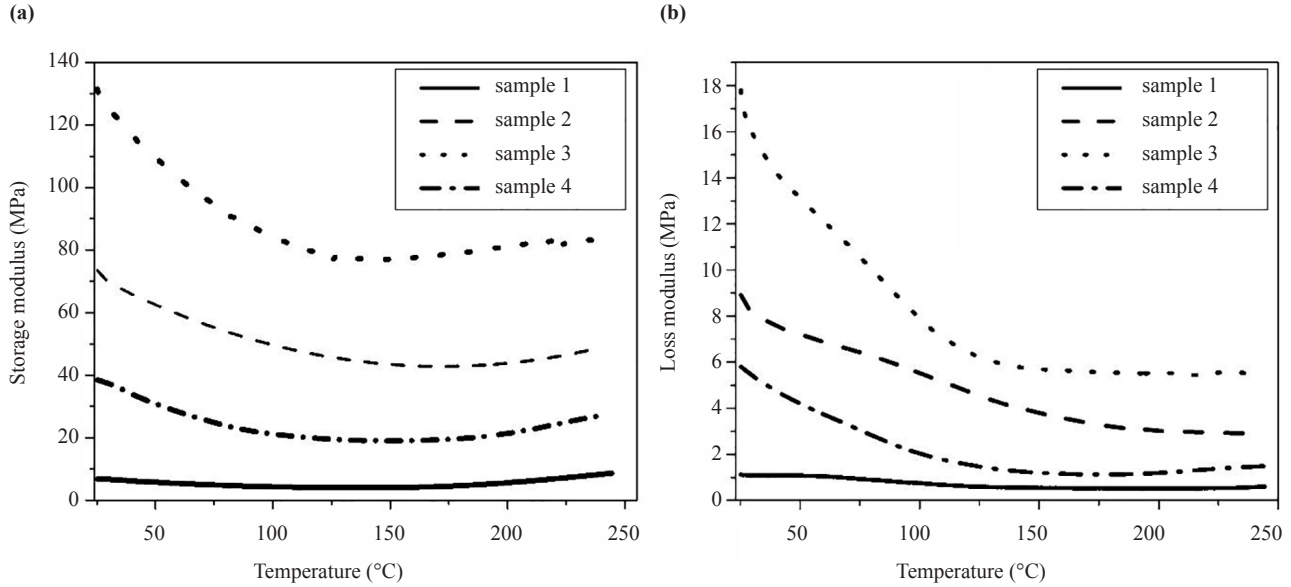

Figure 7. Comparison of (a) storage modulus (b) loss modulus of composites with different fiber content

When there is deformation, loss modulus, reflects the material's capacity to dissipate energy, which is generally in the form of heat or molecular rearrangements. It represents the polymer's viscous character.The higher the incorporated fiber content, the lower the flow property and the higher the loss modulus.[37] However, the composite with 60 w/w fiber content has shown a great decrease in loss modulus due to the absence of tight binding between the fibers and the polymer matrix. The absence of tight binding increases the flow thus lowering the loss modulus. The viscosity of the materials steadily lowers as the temperature rises[37], resulting in an increase in the flow property, as shown in Figure 7(b) by the drop in the loss modulus. After reaching the temperature of 130 °C-140 °C further crosslinking starts and the flow property of the composite decreases.

Thus the 50 w/w (sample 3) is chosen as the optimum fiber content that imparts the maximum strength to the composite. The composite was further modified keeping the fiber content at 50 w/w as shown in Table 2, by changing the content of LO and BPO. Also, the effect of curing time and applying a surface coating of the polymer to an already cured polymer was analyzed. MACO was added to make up to 100 w/w.

Table 2. Composition of the optimized composites with 50 wt. % fiber content

Sample	Sample composition (w/w) %				Curing time (min)
	Fiber content	LO	BPO	MACO [a]	
5	50	10	20	20	30
6	50	20	10	10	30
7	50	10	10	30	60
8	50	10	10	30	30
	The cured composite was coated again with the polymer mixture containing LO, BPO and MACO and re-cured.				

[a] MACO was added to make the mixture total to 100 w/w

Figure 8(a) and (b) show the storage modulus and the loss modulus of the modified samples respectively. Out of the modified samples sample 5 with 50% fibers, 20% BPO and 10% LO and cured for 30 minutes showed the highest storage modulus. A significant difference in loss modulus was not observed in samples 5 to 8 with the temperature. However, sample 5 displayed the highest loss modulus at room temperature.

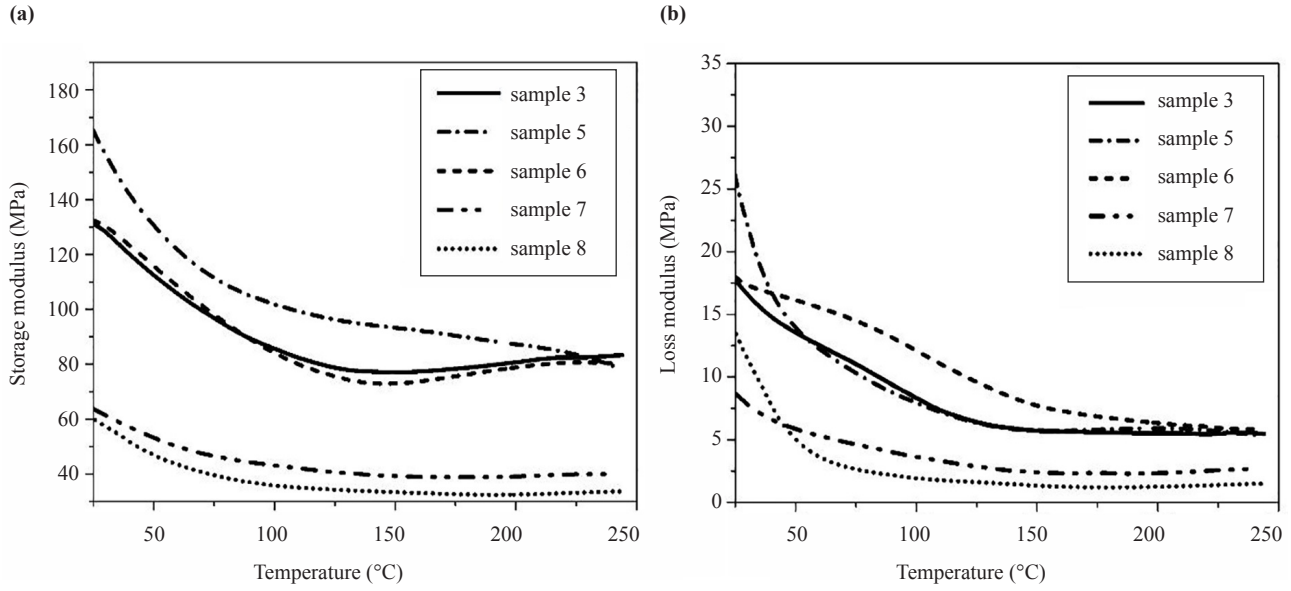

Figure 8. Comparison of the (a) storage Modulus (b) loss modulus of modified composites with 50% fibers (sample 3 & 5-8).

This increase can be attributed to the increase of crosslinking in the presence of surplus free radical initiator which makes the composite more viscous. In sample 6 although there's an excess of LO and the lack of sufficient free radical initiator, BPO may have prevented the further crosslinking of the matrix. Reduction of the storage and loss modulus of sample 7 which is the one-hour cured composite and sample 8 which is the coated composite that underwent curing twice (cured for a total of 1 hour) was due to the decomposition of the composite owing to the prolonged exposure to

heat and pressure.

The composite with the optimum dynamic mechanical properties, which is sample 5 was then analyzed for its tensile and compressive strengths. The stress-strain curve obtained during the tensile testing of sample 5, is shown in Figure 9(a) with the fractured composite in Figure 9(b). The composite exhibited a maximum tensile strength of 16.92 ± 4.70 MPa which is similar to epoxy composite reinforced with short banana fibers and Curaua fiber incorporating high-density polyethylene.[38-39] The Young's modulus of the composite was 5.57 ± 0.03 MPa and the elongation at break was 1.84 ± 0.22 mm while the composite was 2.19 ± 0.06% strained at break.

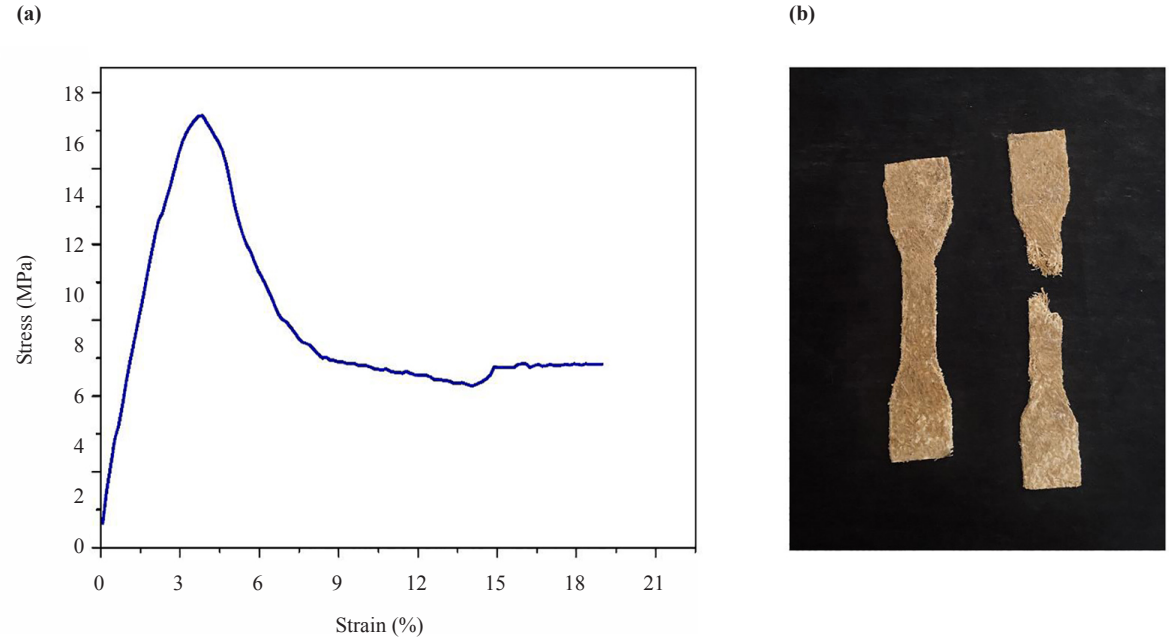

Figure 9. (a) Stress-strain curve of the tensile test and (b) composite before and after the tensile test

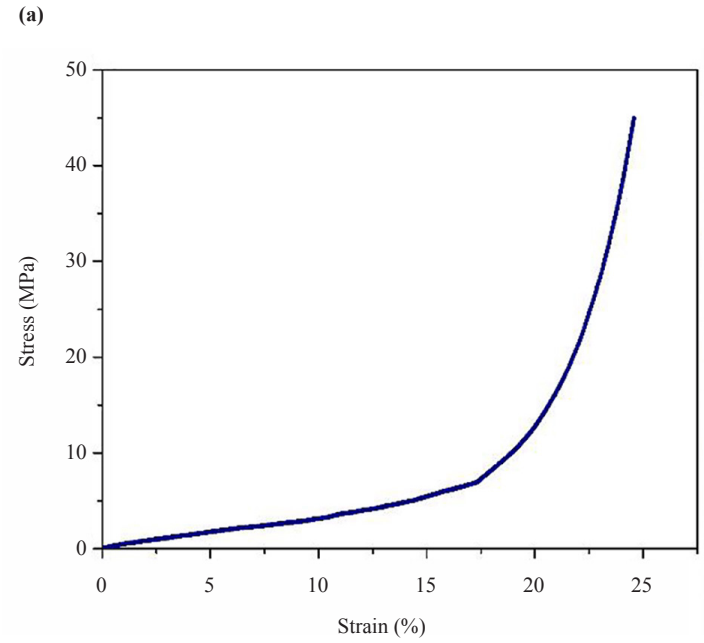

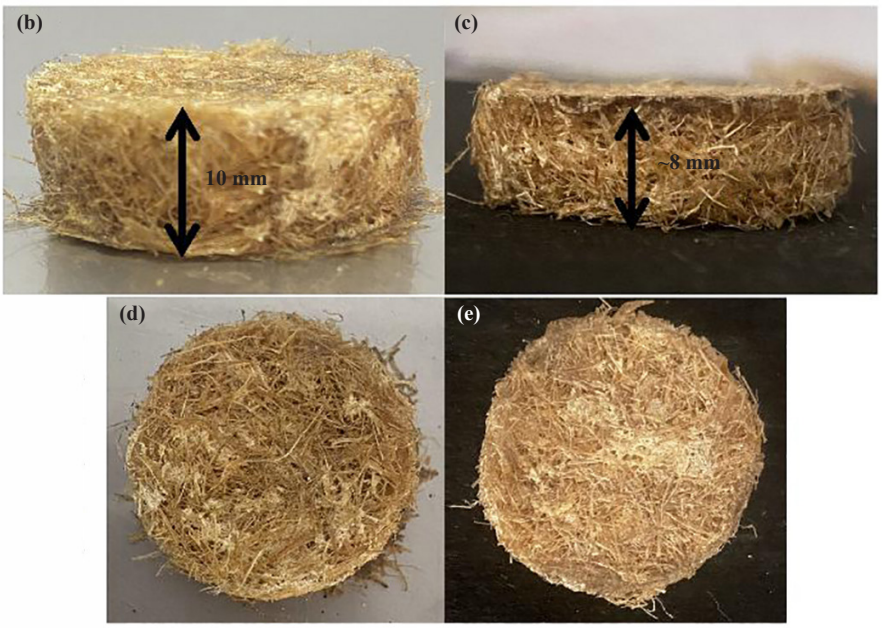

Figure 10. (a) Stress-strain curve of the compressive test, photos of width of the composite (b) before and (c) after, photos of the surface of the composite (d) before and (e) after the compressive test showing no cracks

The stress-strain curve obtained during the compression test of sample 5, with the photos of the composite before and after the test is depicted in Figure 10. The composite didn't show any cracks even after application of a maximum force of 4,500 kN which implies the high resistance of the composite to compressive stress (Figure 10(c) and 10(d)). The strain at maximum stress was 24.72 ± 0.64%.

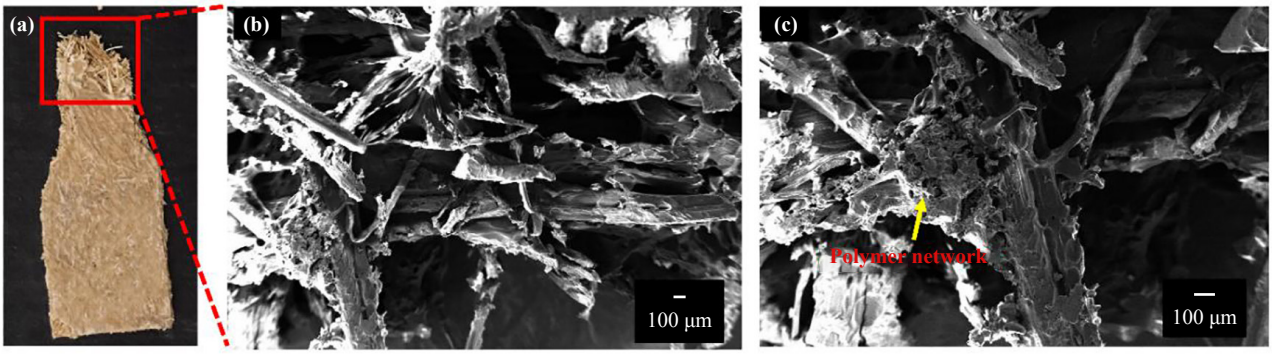

Figure 11. (a) Tensile fractured composite sample, SEM images of tensile fractured surface (b) 50 × magnification and (c) 100 × magnification

From the fractographic analysis using SEM images (Figure 11) it is indicative that there is an inhomogeneity of the polymer network throughout the fractured surface but yet there is a polymer matrix attached to the fiber surfaces. This insufficient interaction between the fiber and the matrix will cause the failure of the composite due to inefficient stress transfer throughout the composite.[40] The short fibers are randomly oriented within the composite. In addition, voids in the polymer network are also visible in Figure 11 (c). Hence the failure of the composite can be a consequence of fiber pulling out, matrix tearing and the poor interfacial bonding in the fiber-polymer matrix.[41-42]

3.4 *Comparison of the water uptake*

Figure 12 (a) and (b) show the percentage water uptake of the samples. It is observed in Figure 12 (a) that the amount of fibers has significantly influenced the water uptake of the composites. With the increase in fiber content, the percent water uptake has increased. This is due to the hydrophilicity of the natural fibers. A significant change in water uptake was not observed in changing the composition of other components of the composite as observed in Figure 12(b). The lowest water uptake percent was shown by sample 8, which was coated with the polymer, as the hydrophobic polymer prevents the inflowing of water into the composite. The percentage of soluble matter in all the composites was 2%-4%. The pH value of the water samples in which the composites were kept was around 3.9 and was assumed due to the leaching out of the acidic substance from the composites.

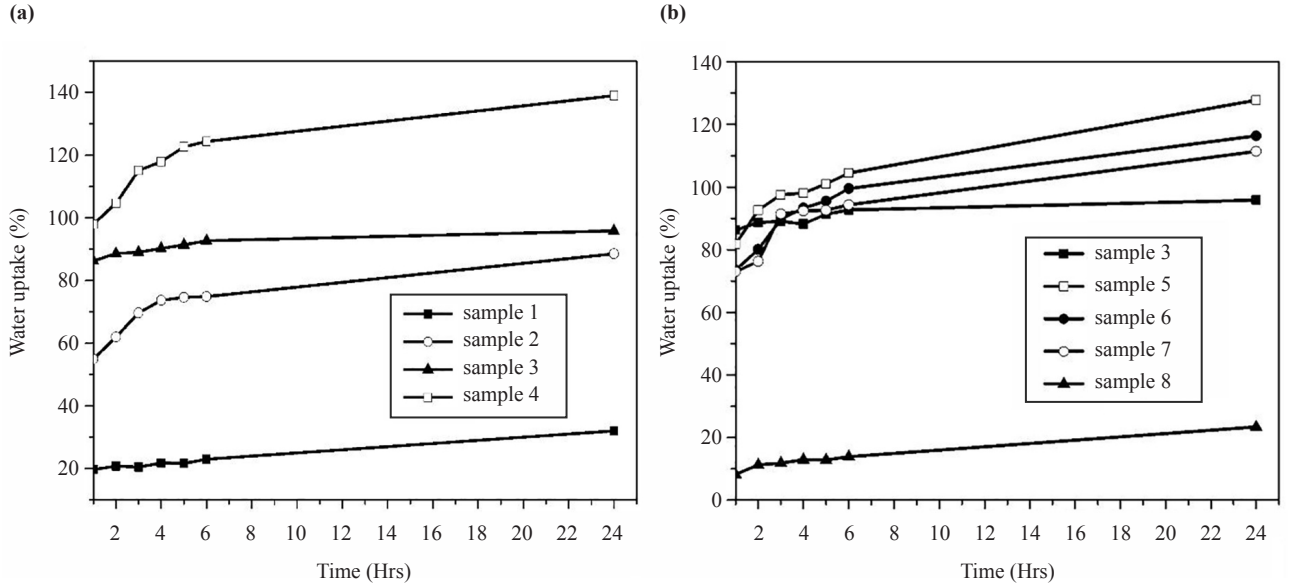

Figure 12. Comparison of water uptake percentage of (a) composites with different fiber content (samples1-4) (b) modified composites with 50% fibers (sample 3 and sample 5-8)

3.5 *Comparison of the chemical resistivity*

Figures 13 and 14 show the swelling percentage of the samples in the acid solution and NaCl solution. The increase of fiber content increased the swelling percentage due to the hydrophilicity of the natural cellulose fibers as depicted in Figure 13(a) and Figure 14(a). Of the modified samples, the swelling percentage was decreased with the increase of both LO and BPO percentages in samples 5 and 6, (Figure 13(b) and 14(b)) and was attributed to the increase of crosslinking density holding the sample together without allowing it to swell. The coated sample had the lowest swelling as its hydrophobic polymer coating resists the entering of acidulated and salted water.

The samples showed very poor resistance to alkaline solution. The samples swelled and finally fragmented into pieces leaving only the fibers when soaked in alkaline solution. Most of the polymer matrix had dissolved in the alkaline solution due to saponification. When considering the chemical swelling of samples 5 to 8, sample 8 which is the coated composite was the most resistant to swelling.

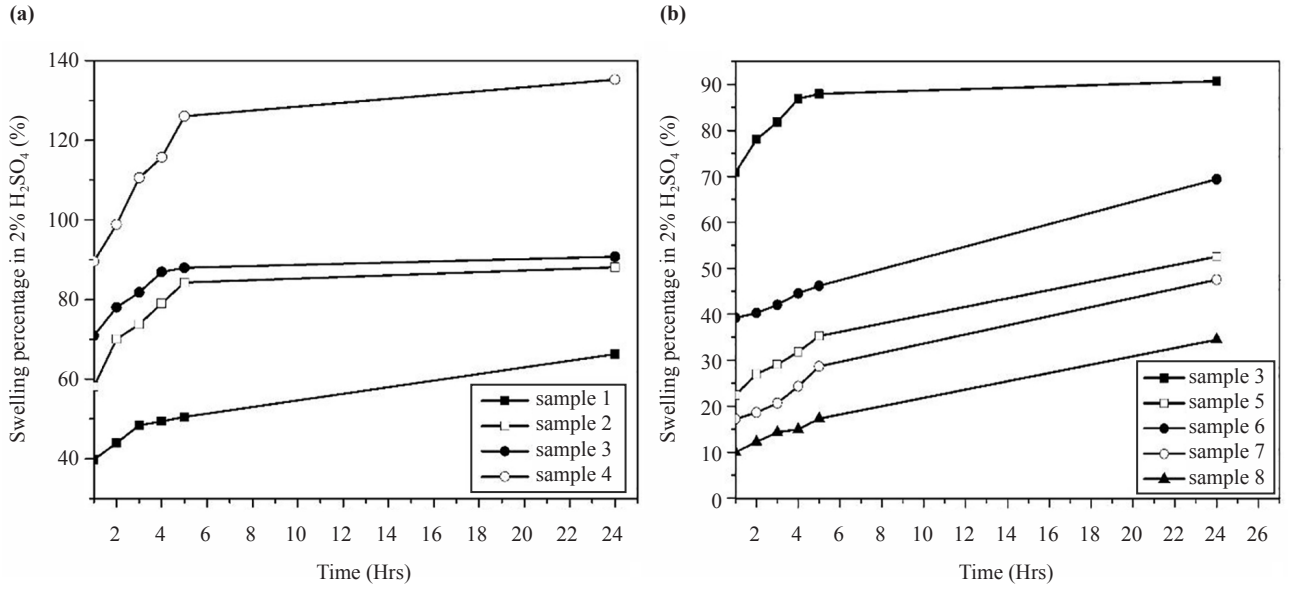

Figure 13. Comparison of acid swelling of (a) composites with different fiber content (samples1-4); (b) modified composites with 50% fibers (sample 3 and sample 5-8)

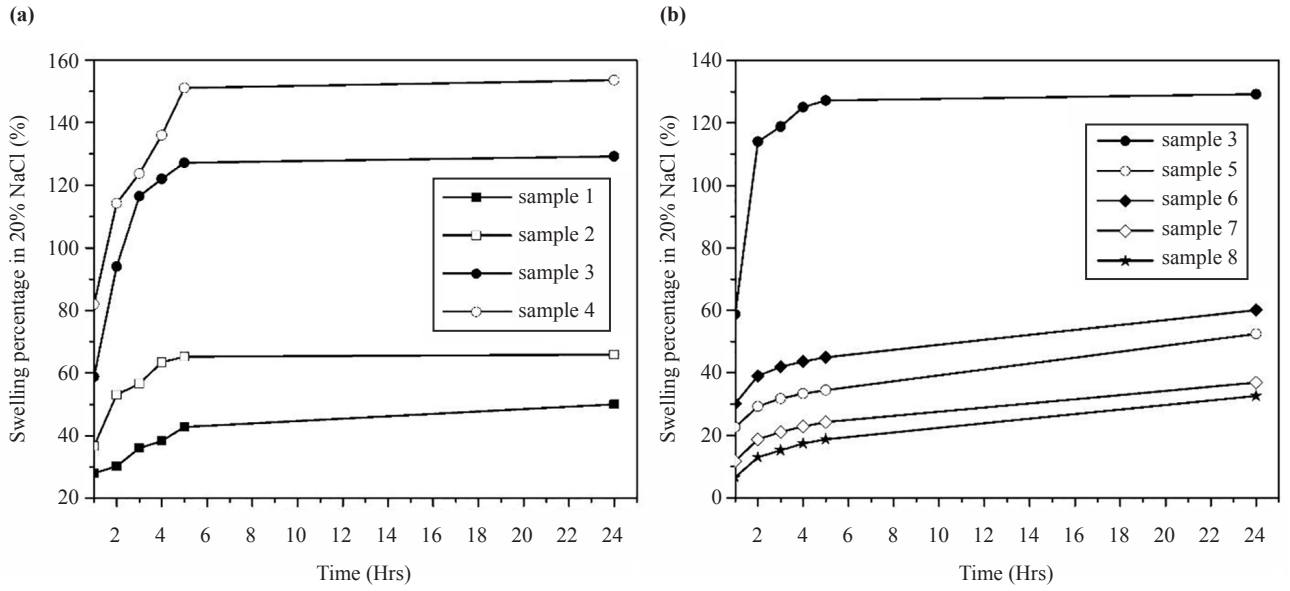

Figure 14. Comparison of swelling in salt, of (a) composites with different fiber content (samples1-4); (b) Modified composites with 50% fibers (sample 3 and sample 5-8)

3.6 *Thermogravimetric and thermal conductivity analysis*

In order to study the thermal stability of the treated banana fibers and the optimum composite (sample 5), TGA was performed and the primary and derivative thermograms (DTG) were recorded (Figure 15(a) and (b)). From the DTG curve, it is evident that two common inflection points (the temperature at which the degradation rate is maximum) resulted around 60 °C and 360 °C for both fibers and composite whereas two additional inflection points around 160 °C and 411 °C are present in the composite. The first peak is around 60 °C which ranges from 39 °C to 110 °C and

represents the loss of absorbed water and other volatiles. The major peak around 360 °C, ranging from 270 °C to 390 °C represents the decomposition of the polymeric network of cellulose, lignin, and a wide range of organic molecules in the fibers and the composite. The major inflection point of the treated fiber appears at 360 °C whereas it is 366 °C for the composite, indicating thermal stability of the composite over the fibers.[17] The weight loss from 140 °C to 190 °C in the composite can be attributed to the loss of low molecular weight oligomers of the polymer composite.[43] The decomposition stage above 400 °C in the composite might be due to the decomposition of MACO and other high molecular weight oligomers of the composite.[44]

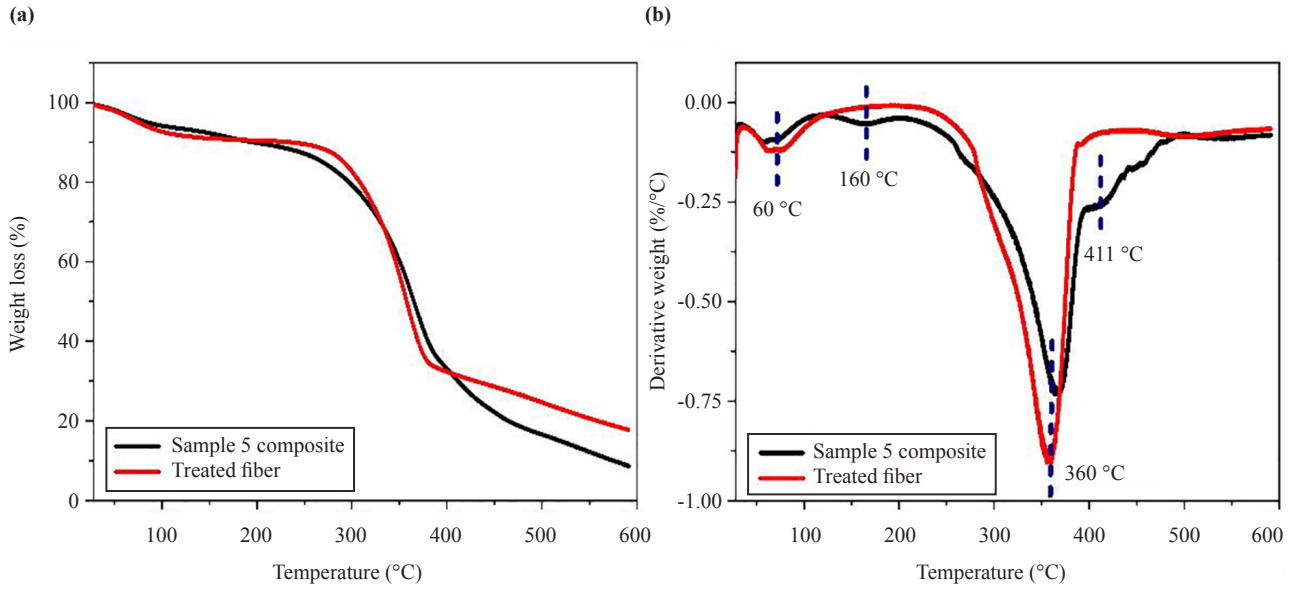

Figure 15. (a) Primary thermograms and (b) derivative thermograms of the sample 5 and treated banana fibers

The sample with the optimum mechanical and chemical properties was tested for its thermal conductivity using a transient plane source (TPS) thermal characterization technique with a hot disc thermal constants analyzer. Thermal conductivity is defined as the amount of heat conducted per unit of time and unit area through a plate of unit thickness. The average thermal conductivity of the composite at room temperature was found to be 0.1883 ± 0.0008 W $m^{-1}K^{-1}$ and the average thermal diffusivity was 0.5012 ± 0.0051 mm^2/s which is similar to that of wood.[45-46] It is evident in many studies that natural fiber composites are thermal insulators and hence, the composite can be used as thermal insulation material.[47]

4. Conclusion

A green polymer composite with a higher percentage of natural resources and post-harvest waste was successfully fabricated in this research endeavor. Particularly the matrix of the composite was developed using maleated castor oil and linseed oil along with NaOH-treated banana fibers as the reinforcing phase. The composite was fabricated by compression molding. The characterization of the fibers and the composites was carried out using FT-IR, XRD, DMA, UTM, SEM, TG/DTG and HDT. Composites were also analyzed for their water absorptivity and chemical resistivity.

When considering only the strength, sample 5 with 50% (w/w) fibers, 20% (w/w) BPO, 10% (w/w) LO, 20% (w/w) MACO and cured for 30 minutes exhibited the highest mechanical properties while it displayed a considerable resistance to swelling in both water and chemicals compared to the other samples. The maximum resistance to swelling in both water and chemicals was shown by sample 8, the coated sample although it had the lowest strength. Hence it can

be concluded that sample 5 with 50% (w/w) fibers, 20% (w/w) BPO, 10% (w/w) LO, and 20% (w/w) MACO and cured for 30 minutes by hot pressing under a pressure of 500 psi showed the optimum mechanical and chemical properties. The maximum tensile strength of the optimum composite was 16.92 ± 4.70 MPa and the composite was resistant against a compressive force of 4,500 kN without any fractures. The composite showed a considerable swelling in water, 20% (w/v) salt water, and 2% (w/v) acidulated water but recovered to their initial states on drying. Composite had poor resistance to 2% (w/v) alkaline solution. The thermal conductivity of the novel composite was similar to that of wood. Hence it can be classified as a thermal insulator.

The fabricated green composite showed potential to replace petroleum-based composites used in domestic applications such as panels and thermal insulators. Additionally, the composite can have potential uses in impact-bearing applications in packaging industries.

Acknowledgement

This work was funded by the University of Sri Jayewardenepura, Sri Lanka. The authors would like to acknowledge the Instrument centres of the University of Sri Jayewardenepura, the University of Moratuwa and the Open University of Sri Lanka for their testing services. We are also grateful to the Faculty of Technology, University of Sri Jayewardenepura for providing DMA testing facilities. Furthermore, the authors would like to acknowledge the Dry Rubber Laboratory, Department of Polymer Science and Technology of the University of Sri Jayewardenepura for their prompt support in sample testing.

Conflict of interest

The authors declare no competing financial interest.

References

[1] Vinod, A.; Sanjay, M. R.; Suchart, S.; Jyotishkumar, P. *J. Clean. Prod.* **2020,** *258*, 120978.
[2] Samir, A.; Ashour, F. H.; Hakim, A. A. A.; Bassyouni, M. *Npj Mater. Degrad.* **2022,** *6*(1), 68.
[3] Thomas, J.; Patil, R. *Ind. Eng. Chem. Res.* **2023,** *62*(4), 1725-1735.
[4] Hamnas, A.; Unnikrishnan, G. *Renew. Sust. Energ. Rev.* **2023,** *182*, 113413.
[5] Akpan, U. G.; Jimoh, A.; Mohammed, A. D. *Leonardo J Sci.* **2006,** *8*(1), 43-52.
[6] Salimon, J.; Noor, D. A. M.; Nazrizawati, A.; Noraishah, A. *Sains Malays.* **2010,** *39*, 761-764.
[7] Mubofu, E. B. *Sustain. Chem. Process.* **2016,** *4*(1), 1-12.
[8] Mistri, E.; Routh, S.; Ray, D.; Sahoo, S.; Misra, M. *Ind Crops Prod.* **2011,** *34*(1), 900-906.
[9] Wang, H. J.; Rong, M. Z.; Zhang, M. Q.; Hu, J.; Chen, H. W.; Czigány, T. *Biomacromolecules* **2008,** *9*(2), 615-623.
[10] Xia, Y.; Larock, R. C. *Green Chem.* **2010,** *12*(11), 1893-1909.
[11] Dutton, H. J.; Cannon, J. A. *JAOCS.* **1956,** *33*(1), 46-49.
[12] Mahmud, S.; Hasan, K. M. F.; Jahid, M. A.; Mohiuddin, K.; Zhang, R.; Zhu, J. *J. Mater. Sci.* **2021,** *56*, 7231-7264.
[13] Arunkumar, S.; GladsonVarghese, A.; Jayaraman, R. *Mater. Today: Proc.* **2023,** 2214-7853.
[14] Rajamanickam, S. K.; Manoharan, M.; Ganesan, S.; Natarajan, P.; Rajasekaran, P. *J. Nat. Fibers* **2022,** *19*(12), 4731-4746.
[15] Kumar T, S. M.; Yorseng, K.; N, R.; Siengchin, S.; Ayrilmis, N.; Rajulu A, V. *Process Saf. Environ. Prot.* **2019,** *124*, 187-195.
[16] Thiagamani, S. M. K.; Nagarajan, R.; Jawaid, M.; Anumakonda, V.; Siengchin, S. *J. Waste Manag.* **2017,** *69*, 445-454.
[17] Kumar, T. S. M.; Rajini, N.; Tian, H.; Rajulu, A. V.; Winowlin Jappes, J. T.; Siengchin, S. *Int. J. Polym. Anal.* **2017,** *22*(5), 415-423.
[18] Di Mauro, C.; Genua, A.; Rymarczyk, M.; Dobbels, C.; Malburet, S.; Graillot, A.; Mija, A. *Compos Sci Technol.* **2021,** *205*, 108678.

[19] Nurchi, C.; Buonvino, S.; Arciero, I.; Melino, S. *Int. J. Mol. Sci.* **2023,** *24*(3), 2153.
[20] Singha, A. S.; Thakur, V. K. *Int. J. Polym. Anal.* **2009,** *14*(4), 301-321.
[21] Pfister, D. P.; Larock, R. C. *Compos. Part A Appl. Sci. Manuf.* **2010,** *41*(9), 1279-1288.
[22] Sharma, V.; Banait, J. S.; Larock, R. C.; Kundu, P. P. *Express Polym. Lett.* **2008,** *2*, 265-276.
[23] Ighalo, J. O.; Adeyanju, C. A.; Ogunniyi, S.; Adeniyi, A. G.; Abdulkareem, S. A. *Compos. Interfaces* **2021,** *28*(9), 925-960.
[24] Pothan, L. A.; George, J.; Thomas, S. *Compos. Interfaces* **2002,** *9*(4), 335-353.
[25] Zin, M. H.; Abdan, K.; Norizan, M. N.; Mazlan, N. *Pertanika J. Sci. Technol.* **2018,** *26*(1), 2231-8526.
[26] Lakshmi Narayana, V.; Bhaskara Rao, L. *Mater. Today: Proc.* **2021,** *44*, 1988-1994.
[27] Geethamma, V. G.; Joseph, R.; Thomas, S. *J. Appl. Polym. Sci.* **1995,** *55*(4), 583-594.
[28] Merlini, C.; Soldi, V.; Barra, G. M. O. *Polym. Test.* **2011,** *30*(8), 833-840.
[29] Corrales, F.; Vilaseca, F.; Llop, M.; Girones, J.; Mendez, J. A.; Mutje, P. *J. Hazard. Mater.* **2007,** *144*(3), 730-735.
[30] Guimaraes, J. L.; Frollini, E.; Da Silva, C. G.; Wypych, F.; Satyanarayana, K. G. *Ind Crops Prod.* **2009,** *30*(3), 407-415.
[31] Bar, M.; Belay, H.; Alagirusamy, R.; Das, A.; Ouagne, P. *J. Nat. Fibers* **2022,** *19*(13), 5956-5973.
[32] Vardhini, K. J.; Murugan, R.; Rathinamoorthy, R. *Indian J Fibre Text Res.* **2019,** *44*(4), 459-465.
[33] Lu, J.; Khot, S.; Wool, R. P. *Polymer* **2005,** *46*(1), 71-80.
[34] Menard, K. P.; Menard, N. R. Dynamic mechanical analysis in the analysis of polymers and rubbers. In *Encyclopedia of Polymer Science and Technology*; Wiley Online Library, 2002; pp 1-33.
[35] Jacob, M.; Francis, B.; Thomas, S.; Varughese, K. T. *Polym. Compos.* **2006,** *27*(6), 671-680.
[36] Chirayil, C. J.; Joy, J.; Mathew, L.; Koetz, J.; Thomas, S. *Ind Crops Prod.* **2014,** *56*, 246-254.
[37] Rezaei, F.; Yunus, R.; Ibrahim, N. A. *Mater. Des.* **2009,** *30*(2), 260-263.
[38] Venkateshwaran, N.; ElayaPerumal, A.; Jagatheeshwaran, M. S. *J. Reinf. Plast. Compos.* **2011,** *30*(19), 1621-1627.
[39] Morais, J. A. d.; Gadioli, R.; De Paoli, M.-A. *Polímeros.* **2016,** *26*, 115-122.
[40] Pothan, L. A.; Oommen, Z.; Thomas, S. *Compos Sci Technol.* **2003,** *63*(2), 283-293.
[41] Alsuwait, R. B.; Souiyah, M.; Momohjimoh, I.; Ganiyu, S. A.; Bakare, A. O. *Polymers* **2022,** *15*(1), 145.
[42] Adhikari, J.; Biswas, B.; Chabri, S.; Bandyopadhyay, N. R.; Halder, S.; Mitra, B. C.; Sinha, A. *Polym. Compos.* **2018,** *39*, E101-E112.
[43] Chulikavit, N.; Huynh, T.; Khatibi, A.; Das, R.; Kandare, E. *Sci. Rep.* **2023,** *13*(1), 17812.
[44] Rosu, D.; Mustata, F.; Tudorachi, N.; Musteata, V. E.; Rosu, L.; Varganici, C. D. *RSC Adv.* **2015,** *5*(57), 45679-45687.
[45] Lagüela, S.; Bison, P.; Peron, F.; Romagnoni, P. *Thermochim. Acta.* **2015,** *600*, 45-51.
[46] Suleiman, B. M.; Larfeldt, J.; Leckner, B.; Gustavsson, M. *Wood Sci. Technol.* **1999,** *33*, 465-473.
[47] Chikhi, M.; Agoudjil, B.; Boudenne, A.; Gherabli, A. *Energy Build.* **2013,** *66*, 267-273.